Thiolysis and Alcoholysis of Phosphate Tri- and Monoesters with Alkyl and Aryl Leaving Groups. An ab Initio Study in the Gas Phase

Guilherme Menegon Arantes* and Hernan Chaimovich

Instituto de Química, Universidade de São Paulo, Av. Lineu Prestes 748, 05508-900, São Paulo, SP, Brasil

Received: November 4, 2004; In Final Form: March 30, 2005

Phosphate esters are important compounds in living systems. Their biological reactions with alcohol and thiol nucleophiles are catalyzed by a large superfamily of phosphatase enzymes. However, very little is known about the intrinsic reactivity of these nucleophiles with phosphorus centers. We have performed ab initio calculations on the thiolysis and alcoholysis at phosphorus of trimethyl phosphate, dimethyl phenyl phosphate, methyl phosphate, and phenyl phosphate. Results in the gas phase are a reference for the study of the intrinsic reactivity of these compounds. Thiolysis of triesters was much slower and less favorable than the corresponding alcoholysis. Triesters reacted through an associative mechanism. Monoesters can react by both associative and dissociative mechanisms. The basicity of the attacking and leaving groups and the possibility of proton transfers can modulate the reaction mechanisms. Intermediates formed along associative reactions did not follow empirically proposed rules for ligand positioning. Our calculations also allow re-interpretation of some experimental results, and new experiments are proposed to trace reactions that are normally not observed, both in the gas phase and in solution.

1. Introduction

Phosphate transfers, essential reactions in living systems,[1] have been investigated extensively in solution[2−4] and in the gas phase[5−7] and computationally.[8−12] The almost exclusive focus of attention of these studies has been phosphate ester hydrolysis, because this reaction is related both to energy biotransformations and to nucleic acid biochemistry. Other phosphate ester reactions are observed in living systems and, although the reaction products can be the same as those formed upon reaction of phosphoesters with water acting as the sole nucleophile, other intermediates are formed. Hence, the study of the influence of the nucleophile, in particular thiols and alcohols, in phosphate transfers is of relevance. These are important reactions, because a large superfamily of enzymes that catalyze the hydrolysis of phosphate esters exhibit a phosphocysteine[13,14] or phosphoserine[15,16] as kinetically competent intermediates formed after nucleophilic attack of the corresponding thiol or alcohol on the phosphorus center of the substrate.

Few conclusive studies on phosphate ester alcoholysis have been published.[2] 2,4-Dinitrophenyl phosphate (2,4-DNPP) solvolysis was studied in anhydrous methanol and ethanol. Solvent substitution can occur on phosphorus or carbon.[17] The activation free energy ($\Delta G^{\ddagger}$) for CH_3O^- attack on phosphorus in 2,4-DNPP dianion was estimated as 23 kcal/mol (25 °C).[17] In aqueous solution, the $\Delta G^{\ddagger}$ for 2,4-DNPP dianion hydrolysis is 29.5 kcal/mol and that for the monoanion is ca. 3 kcal/mol higher.[18] For 4-nitrophenyl phosphate (4-NPP), butanolysis in neat *tert*-butyl alcohol is ca. 1500 times faster with the dianion when compared with the monoanion, because the $\Delta G^{\ddagger}$ (39 °C) is 24.0 ± 0.1 kcal/mol for alcoholysis of the dianion and 28.5 ± 0.9 kcal/mol for the monoanion.[19] For the hydrolysis of 4-PNP, on the other hand, the monoanion is the most reactive species.[19]

Together with observations of inversion of configuration upon reaction of a chiral phosphate in methanol and racemization for the reaction in *tert*-butyl alcohol,[20] these results are consistent with the current mechanistic interpretations for phosphate hydrolysis, described by an A_nD_n mechanism (Figure 1) with a dissociative transition state (TS) or a $D_n + A_n$ mechanism (Figure 1) where metaphosphate (PO_3^-) is diffusionally equilibrated only with a less nucleophilic and sterically crowded solvent such as *tert*-butyl alcohol.[12]

The small or nonexistent participation of the nucleophile in the rate limiting TS for phosphoester solvolysis implies that the mechanism is essentially independent of solvent nucleophilicity and, therefore, that the mechanisms for phosphoester hydrolysis are similar to that of solvolysis in an alcoholic solvent. The monoanion reaction in *tert*-butyl alcohol is slower because a special pathway, with intramolecular H^+ transfer as proposed for the monoprotonated phosphomonoester,[18] is inhibited because the sterically hindered *tert*-butyl alcohol cannot catalyze H^+ transfer via a six-membered ring as proposed for the hydrolysis in water[11,18] and because the pK_a of the unesterified oxygen of the phosphate group increases in this solvent.[19]

Alcohol and HS^- reactions with trimethyl phosphate (TMP) were analyzed in the gas phase.[5,6] No thiolysis on phosphorus was detected, in agreement with ab initio calculations that demonstrate that reaction at the TMP carbon is kinetically and thermodynamically more favorable.[21] In addition, only traces of alcoholysis at phosphorus were observed (less than 2% of the detected products), but no reaction barriers or energies were provided.[5,6]

Some computational studies have addressed the alcoholysis of phosphate esters. Chang and Lim[10] studied the identity reaction of CH_3O^- + TMP (reaction C, Table 1 and Figure 2) and found that attack at carbon is thermodynamically more favorable. The results obtained by these authors contain vibrational thermal and entropic contributions calculated in the harmonic oscillator approximation, which may contain severe errors (see ref 22 for a theoretical explanation and 21 for

* Corresponding author. E-mail: gma@dinamicas.art.br.

10.1021/jp0449556 CCC: $30.25
Published on Web 06/07/2005

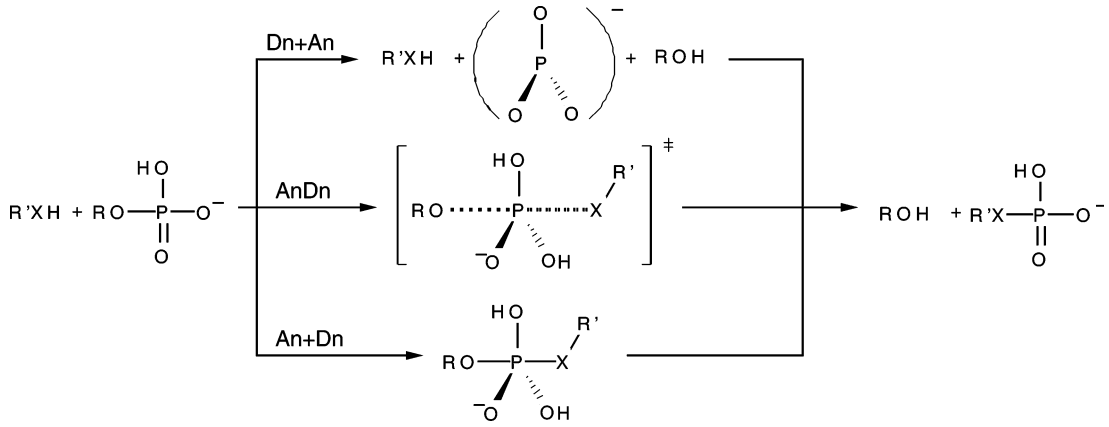

Figure 1. Scheme of the proposed mechanisms[36] for the reactions of phosphate monoesters. Phosphate triesters can ideally react following the same mechanisms.

TABLE 1: Summary of the Phosphate Ester Reactions Studied Here and Previously[a]

reaction	X[a]	R[a]	references
A	S	CH_3	this study and ref 21
B	S	Ph	this study
C	O	CH_3	this study and ref 10
D	O	Ph	this study
E	S	CH_3	this study
F	S	Ph	this study
G	O	CH_3	this study and refs 23,[c] 8, 11, 12, 26
H	O	Ph	this study and 23[c]

[a] Reaction A to D indicate triesters and reactions E to H indicate monoesters. [b] Indicate the groups X and R in Figure 2. [c] Phosphate dianion reaction studied. See text for details.

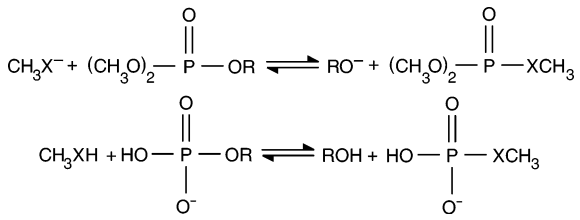

Figure 2. Scheme of the reactions of thiolysis (X = S) and alcoholysis (X = O) of aryl (R = phenyl, Ph) and alkyl (R = methyl, CH_3) phosphate esters.

discussion related to another TMP reaction). In addition, necessary data for ion−molecule complexes and intermediates were not given; hence the calculation of reaction barriers free from thermal and entropic contributions was not possible. We decided to reinvestigate this reaction (Table 1). The associative reactions of CH_3OH with dianionic methyl phosphate ($CH_3OPO_3^{2-}$) and phenyl phosphate ($PhOPO_3^{2-}$) have been investigated.[23] This may be similar to the associative mechanism of reactions G and H (Table 1 and Figure 2) studied here. Differences should appear because calculations of electronic structure of dianions in the gas phase with incomplete basis sets may contain some errors[24,25] and also because the definition of a "reference state" used in ref 23 is not unique and may introduce differences for the reaction in the gas phase. A few other studies[8,11,12,26] have computed the $D_n + A_n$ mechanism of the monoanionic methyl phosphate ($CH_3OPO_3H^-$) reactions (Table 1 and Figure 2). For the sake of completeness, and of trying to obtain a more accurate description, we have also calculated this reaction.

Even fewer studies describe phosphoester thiolysis. The reactivity of *O*,*O*-diphenylphosphochlorothioate, $(PhO)_2P(=S)$-Cl, with several nucleophiles including thiophenoxide, has been described.[27] The reactivity of $(PhO)_2P(=S)Cl$ is, however, very different from the phosphoesters of interest here. The only documented example of phosphoester thiolysis in aqueous solution is the intramolecular reaction of a thionucleotide.[28] This analogue is a phosphodiester monoanion at pH > 2. Assuming that the nucleophile is the thiolate, and correcting the nucleophile concentration using the measured pK_a's for the alcohol and the corresponding thiol analogue, Dantzman and Kiessling concluded that thiolysis is 10^7 times slower than alcoholysis. Hence it appears that thiolates are extremely reluctant nucleophiles toward phosphate esters in aqueous solution.

In the present study, we extend and complement our previous work[21] by first principles computation of reaction profiles for the thiolysis and alcoholysis of a series of phosphate esters (Figure 2 and Table 1). Reactions of tri- and monoesters were computed. Triesters react following a more associative ($A_n + D_n$, Figure 1) mechanism and monoesters are believed to react following a more dissociative ($D_n + A_n$, Figure 1) pathway.[29] The study of triester reactions is also valuable because these reactions do not involve intramolecular proton transfers that influence the intrinsic reactivity of neutral phosphate mono- or diesters. On the other hand, monoesters are the natural substrates of phosphatases.[14,16] Dianionic phosphate monoesters would be more realistic representations of the enzymatic substrates,[14,16] but gas-phase calculations with incomplete basis sets in triple or double negative charged species can be inaccurate.[25,24] The influence of the nature of the leaving group was also examined by computing reactions profiles of alkyl and aryl esters. Some phosphatase subfamilies, namely, the dual-specificity phosphatases,[14,30] catalyze the reaction of both alkyl and aryl phosphate monoesters.

In light of the limited number of quantitative studies on thiolysis and alcoholysis of phosphate esters, reactions A−H (Figure 2 and Table 1) may constitute a reference for the analysis of the intrinsic reactivity of phosphoesters and of the possible catalytic mechanisms of phosphatases, in particular protein tyrosine phosphatases (PTPs).

Details of the ab initio calculations are described in Methods. Reaction energy profiles, structures, and mechanisms are described in Results as well as a simple basis set study and a comparison between calculated and available experimental data, both of which can be used to access the accuracy of the computations. In the Discussion, we analyze the effects of the different nucleophiles, the alkylation state of the ester, and the nature of the leaving group, compare our findings with other computational and experimental studies, and speculate the conclusions that can be drawn from these model reactions.

2. Methods

All computations were carried out for isolated molecules in the gas phase. The pathways of the reactions indicated in Figure 2 and Table 1 were obtained with the 6-31+G(d) atomic basis set[31] for the expansion of the molecular orbitals. The restricted MP2 level[32] (ref 33, Chapter 14) in the frozen-core approximation (ref 33, section 8.3.1) was used to calculate electronic structures, energies and gradients.

The geometries were optimized by the analytic gradient method, using the optimization algorithm developed by Berny Schlegel et al.[34] All the internal coordinates of minima and TSs were optimized. The energy of the stationary points was recalculated in the MP2 level with the 6-311+G(2df,2p) basis set.[35] The resulting electronic and nuclear repulsion energy was defined as E_{MP2}.

Reactions are indicated by a letter accordingly to Table 1 and the mechanisms (Figure 1) are indicated by the IUPAC nomenclature,[36] usually in parentheses. Stationary points such as ion−molecule complexes (IMC), TSs, and intermediates (I) are indicated in the text by a letter corresponding to the reaction (Table 1), followed by the abbreviation of the species. For example, the intermediate of reaction B is indicated by B:I, and the TS of the first step of reaction D is indicated by D:TS1. Two mechanisms are possible for the monoesters reactions. The species in the dissociative mechanism ($D_n + A_n$) are indicated by the letter "d" and, the species in the associative mechanism ($A_n + D_n$), by the letter "a". For example, the TS of the second step of reaction F in the $A_n + D_n$ mechanism is indicated by F:TS2a. Associative reaction pathways are presented in the following sequence: reactants → IMC1 → TS1 → I → TS2 → IMC2 → products. The dissociative reaction occurs in two steps. In the first step, the nucleophile is infinitely separated, and in the second step, the leaving group is infinitely separated. The dissociative reaction sequence is: reactants → TS1 → IMC1 → I → IMC2 → TS2 → products.

Vibrational harmonic frequencies (see ref 37, Chapter 2) were calculated for all the stationary points in the MP2/6-31+G(d) level. Frequencies were obtained analytically for the species in reactions C, E, F ($D_n + A_n$), G, and H ($D_n + A_n$), and numerically, for reactions B, D, F ($A_n + D_n$), and H ($A_n + D_n$). As expected, no imaginary frequency was found for the minimum and only one was found for the TSs.[34] In the vibrational frequency analysis of the stationary points, the lowest 6 real eigenvalues of the atomic mass-weighted Hessian were checked and verified to be smaller than 3 cm^{-1}.[38] Vibrational frequencies were used for calculation of the zero-point energy (ZPE) and vibrational thermodynamic contributions in the harmonic oscillator approximation (see ref 39, section 8.1) for the energy (E_{vib}) and the entropy (S_{vib}) at $T = 298$ K. No empirical scaling was applied to frequencies.[40] Translational (E_{trans} and S_{trans}) and rotational (E_{rot} and S_{rot}) thermodynamic contributions were also obtained in the rigid rotor approximation (see ref 39, section 8.2). Addition of the ZPE to the E_{MP2} resulted in the total energy, E_T.

The intrinsic reaction coordinate (IRC)[41] was calculated[42] from all the TSs in the MP2/6-31+G(d) level. The IRCs corresponded to the expected reaction pathway in the direction of reactants and products.

Electrical dipole moments were calculated by the quantum mechanical dipole operator (see ref 43, pp 150 and 151), applied to the wave functions obtained at the MP2/6-311+G(2df,2p) level. Electronic ionization potentials were obtained from the MP2/6-311+G(2df,2p) energy difference between the closed-shell and the ionized open-shell species in the geometry of the closed-shell molecule; i.e., the calculated ionization is vertical (without nuclear geometry relaxation), with contributions of electronic correlation and relaxation of the molecular orbitals (see ref 43, p 389). The energy of the open-shell species were obtained using the unrestricted method (see ref 33, p 497), with annihilation of the spin contaminants (see ref 43, p 107).

All the above-mentioned computations were carried out with the Gaussian 98[44] program system.

The convergence of the MP2 energy with respect to the basis set size was studied using the 6-311+G set added by polarization functions. The following sets were used: 6-311+G(d), 6-311+G(d,p), 6-311+G(2d,2p), 6-311+G(2df,2p), 6-311+G(2df,2pd), and 6-311+G(3df,3pd). The TZVP and TZVPP basis sets were also used. They are composed by the union of the TZV set developed by Ahlrichs et al.[45] with the polarization functions of the cc-pVDZ and cc-pVTZ sets,[46] respectively. The TZVPP set was the largest one used in this study. Hence, the energies obtained with this set represent the closest values to those that would be obtained with a complete basis set. The energy computations in this basis set study were done with the Gaussian 98 and the Turbomole[47] program systems.

3. Results

Reaction pathways and relative energies for phosphate ester alcoholysis and thiolysis (Figure 2) were obtained. The associative mechanism analyzed here corresponds to the axial conformation, with the oxygen or sulfur nucleophile, the phosphorus electrophile, and the oxygen from the leaving group in line. This conformation is equivalent to the one proposed for the reaction in the PTP active site.[14]

The relative zero of energy for each reaction corresponds to the absolute energy for infinitely separated reactants. Thermodynamic contributions, such as translational, rotational, and vibrational thermal energies (E_{TRV}), as well as the corresponding entropic terms (S_{TRV}), were calculated and are presented in the tables but were *not* added to total energies, E_T.

Optimized geometries of all stationary species, presented in internal coordinates, can be obtained from the corresponding author or from the Internet.[48]

3.1. Phosphate Triesters. In this section, results for reactions A−D (Table 1) are presented. Reaction A was described in an earlier communication where structures of stationary points were shown (Figure 4 in ref 21). These will not be presented again here, but only the recalculated energies (Table 2). Stationary points in reaction B are shown in Figure 7. For reactions C and D, these are shown in Supporting Information Figures 8S and 9S, respectively.

Phosphate triesters can be attacked by nucleophiles at both phosphorus and carbon (alkyl or aryl) centers. Here only attack on phosphorus will be presented because our interest is related to the mechanism of PTP catalysis. We have presented previously an ab initio comparative study of the thiolysis of trimethyl phosphate (TMP + CH_3S^-, reaction A, Table 1) with sulfur attacking on carbon or phosphorus.[21] TMP alcoholysis on carbon has also been described by other groups.[6,10]

The stationary points in reactions A−D exhibit similar conformations and reaction coordinates. Reactant and product IMCs have distorted trigonal bipyramid (TBP) geometries, with attacking and leaving groups in axial position (see B:IMC1 and B:IMC2 in Figure 7). Both equatorial methyl groups are twisted in the direction of the making (or breaking) bond. All intermediates have a TBP configuration. The thiolate and phenoxide groups of the B:I species are equatorial and the methoxide groups are axial (Figure 3). The E_T of the pseudorotamer

TABLE 2: Relative Energies and Entropies in kcal/mol for reaction A[a]

species	ΔE_{MP2}[b]	ΔZPE[c]	ΔE_{TRV}[d]	$T\Delta S_{TRV}$[e]	ΔE_T[f]
TMP + CH_3S^-	0.0	0.0	0.0	0.0	0.0
A:IMC1	−16.3	0.9	1.8	−3.1	−15.4
A:TS1	−0.2	0.9	0.8	−17.3	0.7
A:I1	−4.9	1.2	1.1	−19.9	−3.5
A:TS2[g]	17.1	−0.6	−0.5	−16.7	16.5
A:TS3[g]	16.5	−0.6	−0.5	−16.7	15.9
A:IMC2[g]	12.8	−0.7	−0.1	−8.7	12.1
A:IMC3[g]	13.5	−0.7	−0.1	−10.6	12.8
TMDMP[h]+ CH_3O^-	37.2	−2.7	−2.4	0.1	34.5

[a] Abbreviations for the species names are explained in the third paragraph of the Methods section. [b] Electronic and nuclear repulsion energy calculated in the MP2/6-311+G(2df,2p) level. [c] Zero-point energy obtained in the MP2/6-31+G(d) level. [d] $E_{trans} + E_{rot} + E_{vib}$, thermal energies obtained in the MP2/6-31+G(d) level at 298 K. [e] $S_{trans} + S_{rot} + S_{vib}$, entropies obtained in the MP2/6-31+G(d) level at 298 K. [f] $E_T = E_{MP2} + ZPE$. [g] A:TS3 and A:IMC3 represent structures with sulfur, phosphorus, and leaving group oxygen in line and correspond to TS3b and IMC3b in Figure 4 of ref 21. A:TS2 and A:IMC2 represent structures with sulfur in equatorial position and correspond to TS3a and IMC3a in Figure 4 of ref 21. [h] Thiomethyl dimethyl phosphate.

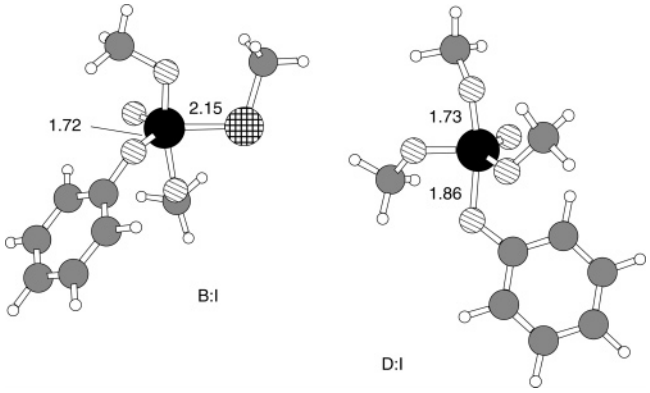

Figure 3. MP2/6-31+G(d) optimized structures for B:I and D:I. Bond distances are shown in ångstroms. Legend for the atomic types: H (white), C (gray), P (black), O (diagonal lines), and S (crossed lines).

containing equatorial methoxides and axial thiolate and phenoxide groups was 3 kcal/mol higher than that of B:I. The phenoxide group in D:I is axial and the methoxide groups occupy equatorial positions (Figure 3). The energy of the pseudorotamer is also 3 kcal/mol higher than the D:I energy. In reaction C, all ligands are methoxides and no conformers were distinguished.

The equatorial methyl groups in B:TS1 are twisted, one in the direction of thiolate and the other in the opposite direction. The C:TS1 (≡C:TS2) and D:TS1 exhibit both equatorial methyl groups twisted in the direction of the methoxide nucleophile (or leaving group for C:TS2). The equatorial groups in B:TS2 and D:TS2 are twisted as in their respective intermediates (Figure 3). The distances between the atoms participating in bond making and breaking, and the imaginary frequencies for the TSs of the triester reactions are shown in Table 6.

Relative energies for each stationary point found are given in Tables 2−5. Reaction A is endothermic and reactions B and D are exothermic. Reaction C is an identity.

The reaction mechanisms for both thiolysis and alcoholysis of the phosphate triesters studied here are associative (A_n + D_n), including the formation of a pentacovalent phosphorus intermediate (Figure 3). For completeness, a $D_n + A_n$ mechanism was also tested. The activation barriers are, at least, 50 kcal/mol higher than those calculated for the $A_n + D_n$ mechanism. For example, the relative energy calculated at the HF/6-31+G(d) level for the breakage of the P−O bond of TMP, corresponding to the first step of a $D_n + A_n$ pathway for reactions A or C, is more than 80 kcal/mol (data not shown here).[49] Hence, no TSs or intermediates in the $D_n + A_n$ mechanism were obtained for phosphate triesters. The dissocia-

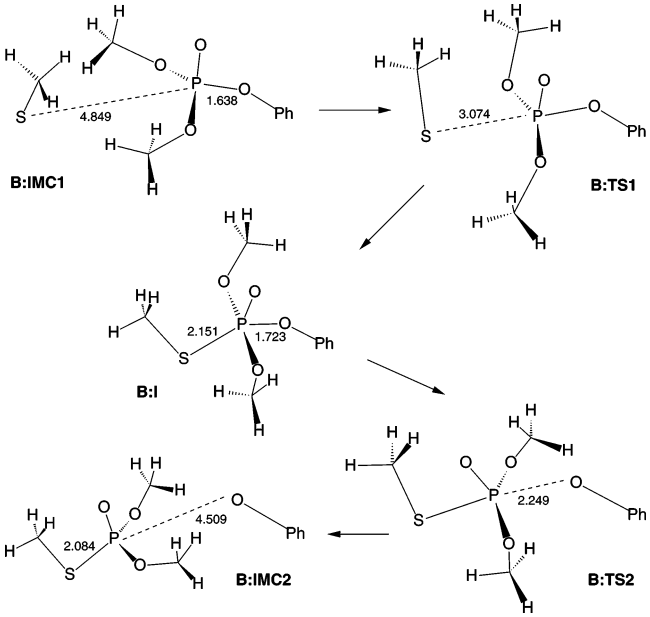

Figure 4. MP2/6-31+G(d) optimized structures for reaction B. Selected distances are shown in ångstroms.

TABLE 3: Relative Energies and Entropies in kcal/mol for reaction B[a]

species	ΔE_{MP2}	ΔZPE	ΔE_{TRV}	$T\Delta S_{TRV}$	ΔE_T
DMPP[b]+ CH_3S^-	0.0	0.0	0.0	0.0	0.0
B:IMC1	−17.4	−0.2	1.0	−7.2	−17.6
B:TS1	−6.5	−0.4	0.1	−11.2	−6.9
B:I	−13.5	−0.2	0.1	−12.6	−13.7
B:TS2	−8.6	−0.6	−0.8	−13.7	−9.2
B:IMC2	−17.4	−0.8	−0.2	−8.1	−18.2
TMDMP + PhO^-	−2.0	0.2	0.2	1.1	−1.8

[a] Abbreviations for the species names are explained in the third paragraph of the Methods section. See Table 2 for the definition of quantities. [b] Dimethyl phenyl phosphate.

TABLE 4: Relative Energies and Entropies in kcal/mol for reaction C[a]

species	ΔE_{MP2}	ΔZPE	ΔE_{TRV}	$T\Delta S_{TRV}$	ΔE_T
TMP + CH_3O^-	0.0	0.0	0.0	0.0	0.0
C:IMC1	−22.5	1.5	2.1	−10.3	−21.0
C:TS1	−16.9	1.4	1.3	−12.7	−15.5
C:I	−32.7	3.2	2.8	−13.9	−29.5
C:TS2	−16.9	1.4	1.3	−12.7	−15.5
C:IMC2	−22.5	1.5	2.1	−10.3	−21.0
TMP + CH_3O^-	0.0	0.0	0.0	0.0	0.0

[a] See Table 2 for the definition of quantities.

TABLE 5: Relative Energies and Entropies in kcal/mol for reaction D[a]

species	ΔE_{MP2}	ΔZPE	ΔE_{TRV}	$T\Delta S_{TRV}$	ΔE_T
DMPP + CH_3O^-	0.0	0.0	0.0	0.0	0.0
D:IMC1	−25.2	0.4	1.1	−9.9	−24.8
D:TS1	−23.5	0.6	0.6	−12.8	−22.9
D:I	−46.2	2.4	2.3	−13.5	−43.8
D:TS2	−42.6	1.8	1.7	−13.1	−40.8
D:IMC2	−53.8	1.8	2.6	−7.7	−52.0
TMP + PhO^-	−39.2	2.6	2.3	0.5	−36.6

[a] See Table 2 for the definition of quantities.

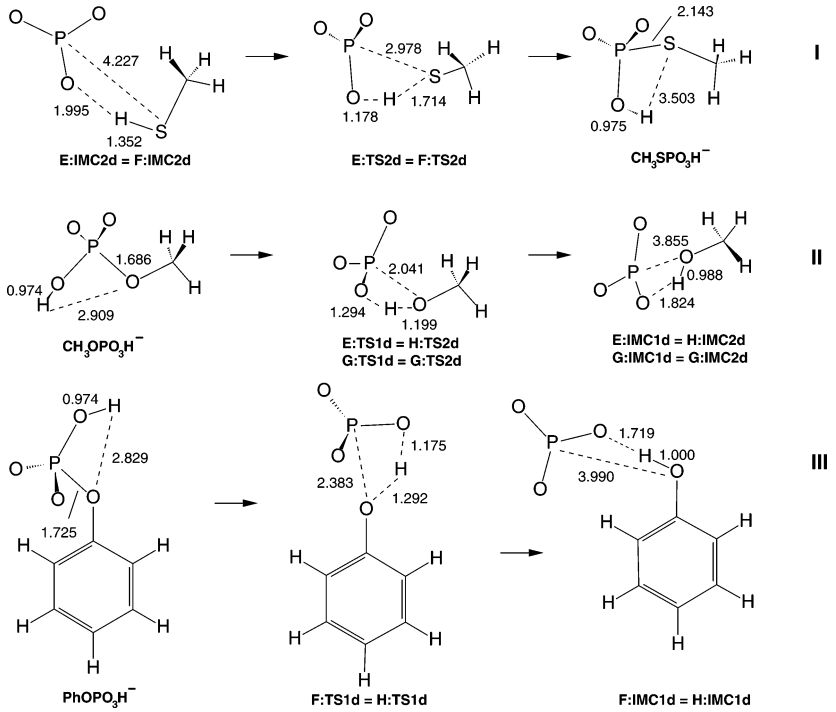

Figure 5. MP2/6-31+G(d) optimized structures for the dissociative reactions. Formation of the P−S bond between thiomethanol and metaphosphate (panel I) and breakage of the P−O bond of either methyl phosphate (panel II) or phenyl phosphate (panel III). Selected distances are shown in ångstroms.

TABLE 6: Caracterization of the TS in the Studied Phosphate Ester Reactions

	TS1		TS2	
reaction	d(P−X)[a]	Im(freq)[b]	d(P−X)	Im(freq)
A	2.802	120i	2.756	114i
B	3.074	100i	2.249	140i
C	2.742	100i	2.742	100i
D	2.931	108i	2.337	116i
E(A_n + D_n)	2.627	112i	2.213	758i
E(D_n + A_n)	2.041	1380i	2.978	1072i
F(A_n + D_n)	2.791	140i	2.283	126i
F(D_n + A_n)	2.383	1047i	2.978	1072i
G(A_n + D_n)	2.274	575i	2.274	575i
G(D_n + A_n)	2.041	1380i	2.041	1380i
H(A_n + D_n)	2.188	650i	2.303	97i
H(D_n + A_n)	2.383	1047i	2.041	1380i

[a] Bond distances in ångstroms between the phosphorus and the nucleophile or leaving group atom, where X = S or O. [b] Imaginary frequency in cm^{-1}.

tive mechanism is considered to be energetically inaccessible in the gas phase.[6]

3.2. Phosphate Monoesters. In this section, the results for the associative and dissociative mechanisms (Figure 1) calculated for reactions E−H (Table 1) are presented. Nucleophiles and leaving groups in the monoester reaction are protonated and the phosphate esters are monoanions (Figure 2). These are the protonation states for reactants and products in the gas phase because the basicity of the nucleophiles and leaving groups is higher than that of the phosphate esters.[6,50−52]

The two steps of the dissociative reaction are independent and the overall reaction results from their union. If one step is the nucleophilic attack on metaphosphate anion yielding a monoester, the same reaction *in the opposite direction* corresponds to the breaking of the ester bond, resulting in dissociated metaphosphate and leaving group. Thus, the dissociative monoester reactions studied here result from the union of only three reactions: formation of the phosphorus−sulfur (P−S) bond between thiomethanol and metaphosphate (panel I, Figure 5) and breakage of the phosphorus−oxygen (P−O) bond of either methyl phosphate (panel II, Figure 5) or phenyl phosphate (panel III, Figure 5). Stationary points for reaction F in the associative mechanism are shown in Figure 6. These points for reaction E, G, and H are shown in Supporting Information Figures 10S, 11S, and 12S, respectively.

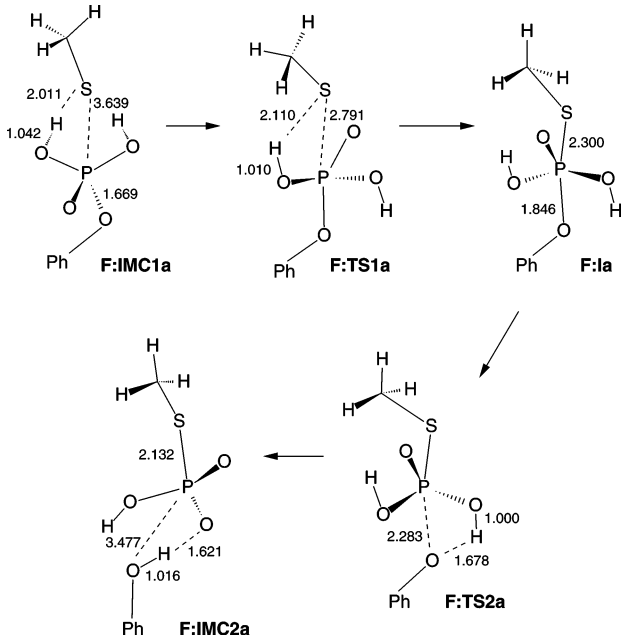

Figure 6. MP2/6-31+G(d) optimized structures for reaction F (A_n +D_n). Selected distances are shown in ångstroms.

The associative IMCs exhibit the hydrogen bonded to the nucleophile (or leaving group) coordinated with one of the ionized phosphate oxygens (see F:IMC1a in Figure 6). The dissociative IMCs show the hydrogen bonded to the nucleophile (or leaving group) coordinated with one of the oxygens of

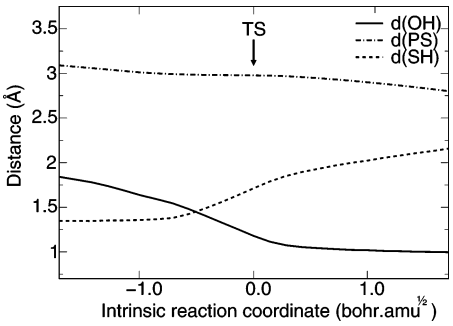

Figure 7. Interatomic distance (see legend) along the IRC of the reaction between CH_3SH and PO_3^-. The TS corresponds to the IRC = 0. The reaction from left to right corresponds to the second step in the reactions E ($D_n + A_n$) and F ($D_n + A_n$).

metaphosphate (Figure 5). The associative intermediates are TBPs with the nucleophile and leaving groups in the axial (in line) position and the phosphate group oxygens (protonated and non bonding) in the equatorial positions (see F:Ia in Figure 6). The dissociative intermediates are composed by three infinitely separated species: metaphosphate in a D_{3h} symmetry, the nucleophile, and the leaving group.

As found in the intermediates, the associative TSs are distorted TBPs with the hydrogen of one of the hydroxides twisted in the direction of the nucleophile (or leaving group) and the other hydrogen twisted in the opposite direction (see F:TS1a and F:TS2a in Figure 6). Dissociative TSs (Figure 5) are complexes with twisted hydrogen bonds and a smaller phosphorus−sulfur bond distance [denoted by d(P−S)] or a smaller phosphorus−oxygen bond distance [d(P−O)]. The breaking (or making) bond distances in the TSs are shown in Table 6.

Two intramolecular H^+ transfers are observed for all monoester reactions: one from the phosphate group to the leaving group and another from the nucleophile to the phosphate group. In the reaction of the triesters, where no H^+ transfer occurs, TSs with imaginary frequencies at ca. 100i cm^{-1} (Table 6) were observed. The imaginary frequencies of the monoesters TSs were in the 100i−1400i cm^{-1} range. Frequencies in the 100i cm^{-1} region indicate TSs with IRCs[41] containing exclusively P−S or P−O bond distances.[41] Frequencies above 1000i cm^{-1} indicate TSs where the IRCs contain only H^+ transfer without contribution of formation (or breakage) of the P−S (or P−O) bond. Intermediary frequencies, around 500i cm^{-1}, are indicative of TSs with contributions of both phosphorus bond formation (or cleavage) and H^+ transfer (Table 6).

As observed previously,[8] the IRCs in the TS regions of $D_n + A_n$ reactions are dominated by H^+ transfers, occurring before bond cleavage (or formation). In the attack of CH_3SH toward metaphosphate (panel I, Figure 5), d(P−S) varies ca. 0.1 Å in the interval $-1.0 < \text{IRC} < 1.0$ bohr·amu$^{1/2}$ (Figure 7). In the same region, the variation of the coordinates indicating H^+ transfer, d(O−H) and d(S−H), was 0.6 and 0.7 Å, respectively (Figure 7). The d(S−H) is practically constant before −1.0 bohr·amu$^{1/2}$. The same is observed for d(O−H) > 1.0 bohr·amu$^{1/2}$. Therefore, H^+ transfer in the reaction between CH_3SH and metaphosphate occurs in a limited interval of the IRC. The behavior of the IRCs for dissociation of $CH_3OPO_3^-$ and $PhOPO_3H^-$ is similar (not shown).[8]

Relative energies for each mechanism and stationary point found are given in Tables 7−10. Reactions E, F, and H are endothermic and reaction G is an identity.

E:TS1a and E:Ia were found to be stationary points of reaction E in the Born−Oppenheimer electronic potential energy surface (PES).[53] The E_{MP2} of E:TS1a was 0.1 kcal/mol higher than the E:Ia intermediate, however, addition of ZPE results in a TS with a lower total energy than the intermediate (Table 7), suggesting that E:Ia is not a stable species and that the associative reaction mechanism is concerted (A_nD_n, Figure 1), with only one TS (E:TS2a).

TABLE 7: Relative Energies and Entropies in kcal/mol for reaction E

species	ΔE_{MP2}	ΔZPE	ΔE_{TRV}	$T\Delta S_{TRV}$	ΔE_T
$CH_3OPO_3H^- + CH_3SH$	0.0	0.0	0.0	0.0	0.0
$A_n + D_n$ Mechanism					
E:IMC1a	−13.9	0.9	1.8	−8.7	−13.0
E:TS1a	11.0	2.4	2.3	−13.0	13.4
E:Ia	10.9	2.7	3.0	−12.3	13.6
E:TS2a	25.0	−0.3	−0.1	−12.4	24.7
E:IMC2a	−15.1	3.1	3.7	−10.7	−12.0
$D_n + a_n$ Mechanism					
E:TS1d	33.3	−2.7	−3.0	−0.8	30.6
E:IMC1d	14.1	−0.4	0.3	2.9	13.7
$CH_3SH + CH_3OH + PO_3^-$	29.0	−1.7	−1.8	11.3	27.3
E:IMC2d	17.4	−0.8	0.0	2.9	16.6
E:TS2d	32.0	−2.8	−2.5	0.5	29.2
$CH_3SPO_3H^- + CH_3OH$	1.9	1.2	1.4	−0.6	3.1

[a] Abbreviations for the species names are explained in the third paragraph of the Methods section. See Table 2 for the definition of quantities.

TABLE 8: Relative Energies and Entropies in kcal/mol for reaction F[a]

species	ΔE_{MP2}	ΔZPE	ΔE_{TRV}	$T\Delta S_{TRV}$	ΔE_T
$PhOPO_3H^- + CH_3SH$	0.0	0.0	0.0	0.0	0.0
$A_n + D_n$ Mechanism					
F:IMC1a	−13.1	0.6	1.0	−10.5	−12.5
F:TS1a	12.7	1.1	1.3	−12.0	13.8
F:Ia	10.0	1.9	2.4	−11.7	11.9
F:TS2a	15.2	1.0	1.3	−11.6	16.2
F:IMC2a	−17.4	1.8	2.7	−8.4	−15.6
$D_n + A_n$ Mechanism					
F:TS1d	32.3	−2.9	−2.9	0.8	29.4
F:IMC1d	10.6	−0.1	0.3	2.1	10.5
$CH_3SH + PhOH + PO_3^-$	33.3	−2.1	−2.2	12.7	31.2
F:IMC2d	21.7	−1.2	−0.3	4.3	20.5
F:TS2d	36.4	−3.2	−2.9	1.9	33.2
$CH_3SPO_3H^- + PhOH$	6.3	0.8	1.0	0.7	7.1

[a] See Table 2 for the definition of quantities.

TABLE 9: Relative Energies and Entropies in kcal/mol for reaction G[a]

species	ΔE_{MP2}	ΔZPE	ΔE_{TRV}	$T\Delta S_{TRV}$	ΔE_T
$CH_3OPO_3H^- + CH_3OH$	0.0	0.0	0.0	0.0	0.0
$A_n + D_n$ Mechanism					
G:IMC1a	−17.3	1.4	2.2	−8.8	−15.9
G:TS1a	19.9	−1.0	−1.1	−12.6	18.9
G:Ia	9.6	2.2	1.9	−13.5	11.8
G:TS2a	19.9	−1.0	−1.1	−12.6	18.9
G:IMC2a	−17.3	1.4	2.2	−8.8	−15.9
$D_n + A_n$ Mechanism					
G:TS1d	33.3	−2.7	−3.0	−0.8	30.6
G:IMC1d	14.1	−0.4	0.3	2.9	13.7
$2CH_3OH + PO_3^-$	29.0	−1.7	−1.8	11.3	27.3
G:IMC2d	14.1	−0.4	0.3	2.9	13.7
G:TS2d	33.3	−2.7	−3.0	−0.8	30.6
$CH_3OPO_3H^- + CH_3OH$	0.0	0.0	0.0	0.0	0.0

[a] See Table 2 for the definition of quantities.

3.3. Basis Set for the Molecular Orbital Expansion. Stationary points for reactions C, E ($A_n + D_n$), and F ($D_n +$

TABLE 10: Relative Energies and Entropies in kcal/mol for reaction H[a]

species	ΔE_{MP2}	ΔZPE	ΔE_{TRV}	$T\Delta S_{TRV}$	ΔE_T
$PhOPO_3H^- + CH_3OH$	0.0	0.0	0.0	0.0	0.0
$A_n + D_n$ Mechanism					
H:IMC1a	−16.9	1.3	1.7	−10.3	−15.6
H:TS1a	20.4	−1.9	−1.9	−12.0	18.5
H:Ia	5.5	1.2	1.2	−12.3	6.7
H:TS2a	7.7	0.6	0.4	−12.6	8.3
H:IMC2a	−22.5	0.8	1.4	−9.2	−21.7
$D_n + A_n$ Mechanism					
H:TS1d	32.3	−2.9	−2.9	0.8	29.4
H:IMC1d	10.6	−0.1	0.3	2.1	10.5
$CH_3OH + PhOH + PO_3^-$	33.3	−2.1	−2.2	12.7	31.2
H:IMC2d	18.5	−0.8	0.0	4.2	17.7
H:TS2d	37.7	−3.1	−3.3	0.6	34.6
$CH_3OPO_3H^- + PhOH$	4.4	−0.4	−0.3	1.3	4.0

[a] See Table *2* for the definition of quantities.

TABLE 11: Hartree−Fock and Second Order Electronic Correlation Relative Energies for Reaction F ($D_n + A_n$) with Respect to the Basis Set[a]

		E_{HF}		$E^{(2)}$	
basis[b]	functions[c]	I[d]	II[e]	I[d]	II[e]
d	130	−0.021	−0.065	0.003	0.015
d,p	172	−0.024	−0.064	0.005	0.020
2d,2p	214	−0.022	−0.062	0.003	0.019
2d,2pd	234	−0.022	−0.062	0.004	0.019
2df,2p	256	−0.022	−0.063	−0.001	0.017
2df,2pd	276	−0.022	−0.063	−0.001	0.017
3df,3pd	318	−0.022	−0.062	0.001	0.017
TZVPP	386	−0.023	−0.062	0.000	0.017

[a] Energy values in atomic unities. [b] Type and quantity of the polarization functions added to the 6-311+G set, excluding the TZVPP set.[45] [c] Total number of basis functions for each species (F:IMC2d, F:TS2d and products). [d] E(products) − E(F:IMC2d), where E is energy. [e] E(products) − E(F:TS2d).

A_n) were chosen as representative for those studied here (Figure 2 and Table 1) and the E_{MP2} of these species was calculated for increasingly larger basis sets. The goal of these calculations was to test the convergence of the electronic energy.

The size of the basis set in the calculations presented here quadruplicate. For the species in reaction C, there are 179 functions in the 6-311+G(d) set and 752 in the TZVPP set (the largest one used in this study). The smallest set, 6-311+G(d), is similar to 6-31+G(d), used for geometry optimization.

For the three reactions studied (Tables 11, 13S, and 14S), the smallest set with a Hartree−Fock (HF) relative energy differing less than 1 kcal/mol from that calculated with the TZVPP set was 6-311+G(2d,2p). For the electronic correlation energy in second-order perturbation,[32] $E^{(2)}$, the difference is smaller than 1 kcal/mol in the 6-311+G(2df,2p) set. The E_T's obtained using the 6-311+G(2df,2p), 6-311+G(2df,2pd), and 6-311+G(3df,3pd) sets differ from that calculated with the TZVPP set in less than 1.2 kcal/mol. This difference was higher than 2.5 kcal/mol using smaller sets.

3.4. Comparison with Experimental Data. As far as we know, no kinetic or thermodynamic experimental data for the gas-phase reactions studied here are available.[5,6]

Table 12 shows available experimental data and calculated values in the gas phase for electronic ionization potentials, dipole moments, geometries, and vibrational frequencies of some of the reactants and products studied here. The calculated structural properties for CH_3OH and CH_3SH are very close to the experimental data. The vibrational frequencies calculated for

TABLE 12: Comparison between Experimental and Calculated Properties in the Gas Phase

species	property[a]	calculated[b]	experimental
TMP	IP	11.8	10.8[67]
	ν(P═O)	1270	1291[68,69]
	ν(P−OC)	1079	1060
	ν(PO−C)	853	866
TMDMP	IP	9.54	9.55[67]
PhOH	IP	8.89	8.75[70]
	dipole	1.45	1.41[71]
CH_3OH	IP	11.36	10.96[72]
	dipole	1.87	1.70[71]
	O−C	1.431	1.425[73]
	O−H	0.972	0.945
	C−H	1.096	1.094
	C−O−H	108.7	108.5
	H−C−O	105.9	107.0
	H−C−H	109.0	108.6
CH_3SH	IP	9.42	9.44[74]
	dipole	1.67	1.52[71]
	S−C	1.816	1.819[75]
	S−H	1.340	1.335
	C−H	1.091	1.091
	C−S−H	96.8	96.5
	H−C−H	109.8	109.8

[a] IP is the ionization potential in eV, dipole is the dipole moment in debyes, ν(X−Y) indicates a vibrational frequency in cm^{-1} and X−Y indicates the bond distances between atoms X and Y in ångstroms, and X−Y−Z indicates the angles between bonds X−Y and Y−Z in degress. The error in the experimental measurements of IP is ±0.3 eV and the errors in the experimental geometries vary, but they are never higher than the last decimal digit shown. Errors for the experimental dipole moments were not available. All ionization potentials are vertical, excluding the TMDMP one. [b] See the Methods section.

TMP are within 2% of the experimental values, and the dipole moments differ by less than 15%. Ionization potentials for TMDMP, PhOH, and CH_3SH are close to experimental ones, but the calculated value for TMP is 1 eV higher. It is noticeable that the calculated properties for sulfur-containing molecules are closer, sometimes identical, to experimental values.

4. Discussion

4.1. Ab Initio Methodology. Analysis of the convergence of the electronic energy as a function of the size of the basis set should be performed with consistently larger sets (see ref 33, section 8.3) such as the cc-pV*X* Z.[46] The computational cost, however, for calculating the electronic structure of compounds such as those used here is very high if $X > 3$. For this reason we fixed the quality of the sets in triple-ζ for the valence electrons (6-311+G set) and tested the effect of adding functions of higher angular momentum. In the absence of significant experimental data for gas-phase alcoholysis or thiolysis of phosphate esters (see above), the energy values obtained using the TZVPP set were taken as references.

For reactions C, E ($A_n + D_n$), and F ($D_n + A_n$), the 6-311+G(2df,2p) was the smallest basis in which the relative HF and $E^{(2)}$ energies differed less than 1 kcal/mol from those calculated using the TZVPP set. The 6-311+G(2df,2p) basis is also used for MP2 energy calculations in the G2 extrapolation scheme.[54]

In the region of P−O and P−S bond formation (or breaking) the PES is relatively rugged; therefore the disposition of equatorial groups influences the geometry optimization of the TSs. For example, in the geometry optimization for reaction A, dihedral angles conditioning equatorial group torsions were combined to the reaction coordinate.[21] Small variations in dihedral angles and in distances of the forming P−S bond resulted in large energy variations, with several local minima

in the PES. We suggested that the observed PES ruggedness was caused by the lack of *N*-electronic flexibility in the wave function expansion.[21] Recent work,[49] including multiconfigurational calculations (ref 33, Chapter 12), natural orbital population,[55] breaking symmetry of an unrestricted electronic wave function,[25] geometry reoptimizations and IRC calculations with an enlarged basis set indicated that the PES ruggedness was determined by the lack of flexibility of the 1-electron basis set, in particular by the absence of diffuse functions in the heavy atoms. This analysis also indicated that one electronic configuration (one Slater determinant) was sufficient to describe the wave functions of the reaction species. We therefore used the 6-31+G(d) set to optimize the geometries in all reactions. We also concluded that inclusion of electronic correlation, at least in second order, must be considered because the calculated HF-level activation energies were up to 18 kcal/mol higher than those obtained at the MP2 level.[11,21]

Comparison of calculated properties with available experimental data was favorable (Table 12),[49] suggesting that the ab initio method employed here for electronic structure calculations, i.e., MP2/6-311+G(2df,2p)//MP2/6-31+G(d), can reproduce experimental observations and has the desired accuracy and capacity for predictions.

As discussed previously,[21] vibrational thermodynamic contributions calculated using the harmonic oscillator approximation can introduce considerable errors in the calculations,[22] notably for the low-frequency vibrational modes. Thus, the computed E_T contain only nuclear repulsion and electronic contributions (E_{MP2}) and ZPE. Accurate values of total energy at 0 K may be more useful than including imprecise thermal and entropic contributions.

No basis set superposition error (BSSE) corrections were used for the reactions studied here.[56] For reaction A, using the 6-311++G(d,p) basis set, the BSSE of the reactant and product complexation was estimated to be 1/8 of the energy values. We expect that complexation energies should have a BSSE even smaller when the 6-311+G(2df,2p) set is used. Errors of such magnitude should not affect the conclusions.

4.2. Factors Determining the Reaction Energies, Barriers and Mechanisms. Energies for triester intermediate formation vary from −19 to +12 kcal/mol. Energies for monoester intermediates formation are relatively higher, varying from 24 to 28 kcal/mol for $A_n + D_n$ mechanisms and from 27 to 31 kcal/mol for $D_n + A_n$ pathways. Hence, intermediate formation in monoesters, and therefore, two-step mechanisms, are not favored. We note that the formation energies for dissociative intermediates were calculated by taking as reference the isolated reactants whereas those for associative intermediates took the previous IMC as reference. These two (different) calculation schemes were used to eliminate, as far as possible, the influence of species complexation and the BSSE.[56,57]

For the triesters reactions, the reaction energy depends strongly on the leaving group and nucleophile. Reaction energies for dissociation of methoxide requires ca. 36 kcal/mol more than dissociation of phenoxide. Thiolysis reaction energies are ca. 35 kcal/mol higher than alcoholysis energies. For the monoesters, H^+ transfer to or from phosphate neutralizes the charge being formed in the reactive groups. Hence, reaction energies are rather insensitive to the nature of the leaving group and the nucleophile.

Two types of mechanisms were calculated for monoester reactions (Figure 1). The differences between barrier heights calculated for the $A_n + D_n$ and $D_n + A_n$ pathways are, at most, 7 kcal/mol, as observed for reaction E. In this reaction the $D_n + A_n$ mechanism has the smallest total barrier. For reaction F, activation of F:TS1d may be competitive with activation of F:TS2a. However, the $A_n + D_n$ pathway should be preferred because its total barrier is 4.5 kcal/mol lower than the $D_n + A_n$. For reaction G, the barrier for G:TS1a activation is 5 kcal/mol higher than the rate-limiting step in the $D_n + A_n$ pathway. Therefore, the $A_n + D_n$ pathway, and G:Ia should not be observed in the gas phase. For reaction H, the $A_n + D_n$ and $D_n + A_n$ pathways exhibited similar total barriers and should be competitive. In summary, the rate-limiting step of monoester reactions is nucleophile addition for reaction H and leaving group dissociation for reactions E−G.

For the triesters, calculations indicate that all reactions proceed via $A_n + D_n$ pathways and that the formation of dissociative intermediates is energetically forbidden. The rate limiting step is the nucleophilic attack in reaction B and the leaving group dissociation in reactions A, C, and D. The barriers for nucleophilic attack are significantly different for alcoholysis and thiolysis, with smaller barriers by 9−11 kcal/mol for alcoholysis.

The main factor determining the mechanism is the phosphate group alkylation state. However, monoesters do not react exclusively by dissociative mechanisms, as currently accepted.[2−4,29] Florián and Warshel used electronic structure calculations to propose that monoesters could also react by associative pathways in solution[8,23]

Nucleophile and leaving group basicity is the second factor determining the mechanism. Hence the interpretation of linear free energy relationships (LFER) of monoester reactions must be taken with caution. The height of the calculated barriers for CH_3OH attack or dissociation are always related to the energy cost of H^+ transfer due to the basicity of methoxide. Therefore, the mechanism of monoester reactions where the attacking or leaving group is CH_3OH will correspond to that minimizing the energy in the H^+ transfer step. Reaction F does not involve CH_3OH and exhibits the lowest activation barrier among the monoester reactions studied here. Experimental results obtained for dianionic monoester hydrolysis in several solvents also indicate that the reaction mechanism can depend on the basicity of the leaving group[18,58] as well as a possible intramolecular H^+ transfer.[11,12,18]

All reactions involving monoesters contain two H^+ transfers along the pathway. These steps significantly alter reaction thermodynamics and kinetics when a comparison is made with the triester reactions. In solution, the presence of a catalyst for H^+ transfer (e.g., water) can lower the barrier for $CH_3OPO_3H^-$ dissociation by ca. 10 kcal/mol.[11,12] Furthermore, the formation of a six-membered ring containing a water molecule facilitates H^+ transfer in monoanion reactions.[11,12,18] This catalytic mechanism is not observed for associative pathways in $CH_3OPO_3H^-$ hydrolysis.[11] Hence, it is likely that the $D_n + A_n$ pathway, already favoured in the gas phase for $CH_3OPO_3H^-$ alcoholysis and thiolysis, should be observed in aqueous solution.[11,12]

4.3. Relation to Experimental Observations. Structures formed along the associative reaction pathways exhibit the phosphorus ligand atoms coordinated at the positions of a TBP (Figure 3). The phosphorus and the equatorial ligands are approximately coplanar in the intermediates and exactly coplanar in C:I and G:Ia, because these reactions are symmetrical. The spatial arrangement of the TBPs are typical of previously proposed intermediates for phosphate ester reactions[2,4,29] and have been observed experimentally in pentacoordinated and hypervalent phosphorus (*V*) compounds called phosphoranes.[4,59] The position of the groups in some of the optimized intermedi-

ates did not obey the (empirically proposed) rules for group arrangement in the TBP.[4,60] According to Pearson (ref 61, Table F.3), ligand electronegativity (χ) follows the order $\chi_{HO} > \chi_{CH_3O} > \chi_{PhO} > \chi_{CH_3S}$. Intermediates D:I, E:Ia, F:Ia, G:Ia, and H:Ia have ligands of lower electronegativity, e.g., PhO^- and CH_3S^-, in axial positions, whereas the above-mentioned rules would suggest that this position should be occupied by the more electronegative groups. Phenoxide in D:I occupies an axial position in the TBP, contrary to the rule that suggests that π-electron donor groups should be equatorial. In reaction A, barriers for methoxide dissociation were similar, with CH_3S^- occupying either the axial (A:TS3) or equatorial (A:TS2, Table 2)[21] positions, suggesting that the relative position of the nonreacting groups in the TBP does not influence reaction barriers. In conclusion, the calculations suggest that the empirical rules for ligand positioning are not followed for the intermediates formed in alcoholysis or thiolysis of phosphate esters in the gas phase.

It has been proposed that energetic barriers are involved in the pseudorotation for conformer interconversion and may preclude intermediate decomposition (or formation) of phosphate esters.[6,60,62] Pseudorotations were observed in the associative reactions (for example, in reaction A, between species A:TS1 and A:I1),[21] but no appreciable activation barriers were detected. We did not search for reaction pathways or TSs for pseudorotamer interconversion; however, if the heights of these barriers are similar to the energy difference between pseudorotamers, 3 kcal/mol for the triester reactions (see Results), the interconversion should not be energy costly. The pseudorotation barrier for the pentacoordinated intermediate of the reaction OH^- + TMP, obtained by electronic structure calculations, is <1 kcal/mol.[10] Taken together these data show that pseudorotamer interconversion is not a mechanistically important process and should not present barriers for phosphorane reactions in alcoholysis or thiolysis.

The only phosphorane that could be observed experimentally is C:I, because its decomposition barrier is high and its formation is exothermic (Table 4). The methodology used in an experimental study of the reaction of TMP with several nucleophiles in the gas phase allows anionic intermediate(s) detection and, because no phosphorane was reported,[6] nucleophile addition to TMP was proposed to be rate limiting.[6] Deuterated $C_2D_3H_3O_4P^-$, a measure of CD_3O^- attack on phosphorus, was detected in very small amounts (only 1.5% of the total detected product). Lum and Grabowski[6] note that phosphorane formation would result in a higher incorporation of CD_3O^- into the products, because the intermediate could decompose to TMP-d_3 and be attacked again by CD_3O^-, yielding $C_2D_6O_4P^-$, which was not detected. The calculated energy profile for reaction C suggests another interpretation for these experimental results. The barrier for the total reaction corresponds to that for intermediate decomposition. CD_3O^- addition to TMP is ca. 10^7 times faster than the rate of leaving group dissociation (Table 4). The low quantity of experimentally detected product may be attributed to the fact that the total barrier for attack on phosphorus in TMP is higher than that for attack on carbon. Moreover, attack on carbon is thermodynamically favored.[10] Observing the formation of the doubly deuterated product is unlikely because the barrier for reaction on phosphorus has to be crossed *twice* with no concurrent attack on carbon or CD_3O^- dissociation. The quantity of $C_2D_6O_4P^-$ formed in this way may be below the experimental detection limit (0.2% of the total reaction product[6]).

From all the reactions studied here, the lowest barrier was calculated for DMPP alcoholysis (reaction D, Table 5). This reaction should be observed experimentally because the barrier for the competitive alcoholysis on the alkyl carbon can be estimated in ca. 8.5 kcal/mol.[63] The reaction barrier for DMPP thiolysis (reaction B, Table 3) is small, and this reaction also should be observed experimentally. The calculated barrier for CH_3S^- attack on the alkyl carbon is 12.6 kcal/mol.[21] Therefore, substitution on carbon and phosphorus should be competitive. Nucleophilic attack on aromatic carbon is less probable in both alcoholysis and thiolysis. We suggest that significant attack on phosphorus should be observed in the gas phase if phosphate triesters with an aryl-derived leaving group react with CH_3O^- or CH_3S^-, differently from what has been described for alkyl triesters.[5,6]

The reaction of HS^- + TMP, experimentally studied in the gas phase, is totally regioselective and the nucleophile only attacks at carbon.[6] The calculated energy profile for reaction A (Table 2) suggests that thiolysis on phosphorus is not observable because the reaction is thermodynamically unfavorable ($\Delta E_{reac} > 30$ kcal/mol), shows a high barrier for elimination of the leaving group and a low barrier for decomposition of the intermediate back to reactants (4.2 kcal/mol, Table 2). Lum and Grabowski[6] and Chang and Lim[10] proposed that the rate limiting step for attack at the phosphorus center in triesters is nucleophile addition. That is the case only for reaction B. Therefore, nucleophilic attack may be rate limiting in some cases, but leaving group dissociation usually presents the highest barrier.

No rate constants have been reported for nucleophilic attack on phosphorus using TMP as a substrate in the gas phase.[5−7] The only experimental value that can be compared with the barrier heights calculated here is the relationship between rate constants for attack on phosphorus and carbon in the reaction of CD_3O^- + TMP. This relationship is equivalent to an energy difference of 2.2 kcal/mol, where reaction at carbon is faster.[6] The estimated barrier for CH_3O^- attack on the TMP carbon is 8.5 kcal/mol[63] and that for attack on phosphorus is 14.0 kcal/mol (Table 3). Consequently, the calculated barrier difference is 3.3 kcal/mol above the experimental one. This proximity demonstrates that the calculations presented here have semiquantitative prediction properties. The disagreement can be attributed to the following sources: lack of accurate thermal (ΔE_{TRV}) and entropical (ΔS_{TRV}) contributions in the calculated values; experimental error, because the observation of the products for attack on phosphorus is close to the detection limit;[6] assumption that the reaction mechanism is A_nD_n, used to calculate the ratio between the rate constants from the measured product distribution;[6] level of the electronic energy calculation [MP2/6-31+G(d)//HF/6-31+G(d)] used in the determination of the relative energy of the TS for attack on carbon.[10] The error associated with the computation of ΔE_T in the barrier for attack on phosphorus should be smaller than the mentioned sources. This comparison involves differences between relative values ($\Delta\Delta E$). Thus, the final uncertainty is the sum of the individual uncertainties for each of the values used.

In aqueous solution, some restricted data for comparing alcoholysis and thiolysis of phosphoesters are available.[28] The rate constant for intramolecular alcoholysis of aryl phosphate diester in aqueous solution is 10^7 times higher than that for thiolysis of a related compound, corresponding to a $\Delta\Delta G^{\ddagger} =$ 9.5 kcal/mol at 25 °C.[28] When these reactions are compared, the effect of the solvent in the relative free energy differences ($\Delta\Delta G$) should largely cancel, because the reaction is intramolecular and the solvent structure around both derivatives (alcohol and thiol) should be similar. Given the limits of this comparison, we found good agreement between experiment and the calcu-

lated difference in barrier height for reactions B and D in the gas phase, $\Delta\Delta E_T = 7.7$ kcal/mol. Both alcoholysis and thiolysis of phosphate di- and triesters should follow a similar (associative) reaction mechanism.[4,29]

The low decomposition barriers, and consequently the reduced half-life of the intermediates formed, in the associative reactions D−F and H suggest that the kinetic observables of these reactions that follow an $A_n + D_n$ pathway should be equivalent to a concerted mechanism (A_nD_n, Figure 1). It is noticeable that experimental measurements of solution reactions of phosphate di- and triesters with activated leaving groups (e.g., phenol derivatives) such as LFER or kinetic isotope effects are traditionally taken as evidences for A_nD_n pathways with "partial" bond formation between the nucleophile and phosphorus in the rate-limiting TS.[2,3,4,29,64]

The calculated barrier for water attack on metaphosphate yielding $H_2PO_4^-$ in aqueous solution is 4.5−5.5 kcal/mol.[11,12] To this value has to be added −2.4 kcal/mol to correct for the difference in standard state (1 M in the calculation) and the molar concentration of liquid water. The calculated barrier for CH_3OH attack on metaphosphate yielding $CH_3OPO_3H^-$ in aqueous solution is 6−8 kcal/mol[11,12] (compare with the 17 kcal/mol barrier in the gas phase, Table 9). The barrier for CH_3SH attack toward metaphosphate yielding $CH_3SPO_3H^-$ in aqueous solution can be estimated as 7 kcal/mol on the basis of the activation energy in the gas phase (13 kcal/mol, Table 7) and a lower solvation energy for species derived from CH_3SH in comparison to those derived from CH_3OH. Therefore, water addition to metaphosphate should be faster than addition of CH_3OH or CH_3SH, and PO_3^- diffusion in aqueous solution.[65] Also, neither alcoholysis nor thiolysis of phosphate monoesters should be observable in aqueous solutions because metaphosphate can be rapidly, and selectively, captured by a water molecule of the hydration sphere.[12]

It is attractive to speculate, however, that monoester thiolysis should be observed in a sterically crowded nonaqueous solvent such as *tert*-butyl alcohol. Solvolysis of a chiral phosphomonoester in *tert*-butyl alcohol results in racemization, indicating that the half-life of metaphosphate is sufficiently long to allow diffusion and equilibration before reaction with the solvent.[20] Under these conditions it is likely that a better nucleophile, such as CH_3SH, could react with PO_3^-.

5. Conclusions

The study of convergence of electronic energy with the enlargement of the basis sets demonstrated that the relative energies obtained with the 6-311+G(2df,2p) set differed by less than 1 kcal/mol of those obtained with the largest set, TZVPP. Most of the calculated properties were close to the available experimental data, demonstrating the adequacy of the level used in the calculations [MP2/6-311+G(2df,2p)//MP2/6-31+G(d)].

In the TS region, the IRCs of the associative reactions of phosphate triesters were dominated by phosphorus bond formation or breakage whereas in the monoesters dissociative mechanisms, the dominant coordinate involved H^+ transfer.

Reactions of phosphate triesters with oxygen and sulfur nucleophiles follow an $A_n + D_n$ mechanism. In phosphate monoesters, the reaction mechanism can vary with the nature of the nucleophile and with the type of leaving group. Thiolysis of methyl phosphate should follow a $D_n + A_n$ mechanism, with a barrier that is ca. 7 kcal/mol lower than that of the $A_n + D_n$ pathway. The mechanism of phenyl phosphate thiolysis, on the other hand, should be $A_n + D_n$, with a barrier that is ca. 4.5 kcal/mol lower than that of the $D_n + A_n$ pathway. Methanolysis of methyl phosphate, an identity reaction, follows a $D_n + A_n$ mechanism that has a barrier ca. 4.2 kcal/mol lower than the associative pathway whereas, for methanolysis of phenyl phosphate, both pathways are energetically equivalent.

Stable intermediates with TBP geometry can be formed in associative mechanisms in phosphate esters reactions. However, the empirically proposed rules for ligand positioning[4,60] are not respected and pseudorotations are not important for these reactions.

The main factors controlling thermodynamics, kinetics, and mechanisms are, in order of relative importance, the esterification of the phosphate group, nucleophile and leaving group basicity, and the possibility of H^+ transfer during reaction. Barriers and reaction energies calculated for phosphate tri- and monoesters are significantly different. Monoester reactions are always endothermic. For triesters, reaction energies vary significantly (70 kcal/mol) with leaving group and nucleophile. With the exception of reaction A, barriers for triester reactions are lower than 16 kcal/mol and are smaller than the barriers calculated for monoesters, which exceed 28 kcal/mol.

The geometries and energy profiles are altered when methoxide or methanol are a reactant (or product) because of their basicity. Phenol, which is less basic, distorts the geometry to a lesser extent and, as expected, is a better leaving group.

The reactions described here can be analyzed as possible models for PTP catalysis. A decrease in the electrostatic repulsion between the ionized nucleophile in the active site and the dianionic substrate[14] is a possible source of catalysis by PTPs. This effect can be estimated in ca. 10 kcal/mol.[66] Formation of a stable intermediate, phosphorane or metaphosphate, must be catalyzed by PTPs, because these intermediates in monoester reactions exhibited formation energies higher than 24 kcal/mol. It is possible, therefore, that the enzyme catalytic mechanism is A_nD_n and thiolysis at the active site occurs in a single step without the formation of stable intermediates. Another possible catalytic source, which has been identified experimentally in PTPs is the protonation of the leaving group.[14] This is related to the present findings for monoester reactions, particularly when CH_3OH is the leaving group.

Because alcoholysis and thiolysis of phosphate esters are not easily observable in aqueous solution, the set of reactions analyzed here is a reference for studying phosphate reactivity with these nucleophiles.

Acknowledgment. G.M.A. thanks Prof. Peter R. Taylor (University of Warwick, U.K.) for the hospitality during a recent visit to his group and for providing part of the computational resources used in this work. A fellowship (G.M.A.) and financial support from FAPESP (Fundação de Amparo a Pesquisa do Estado de São Paulo) are also acknowledged.

Supporting Information Available: Five figures showing the MP2/6-31+G(d) optimized structures for reactions C−E, G, and H in the $A_n + D_n$ mechanism and two tables showing the relative energies for species in reactions C and E with respect to different basis sets. This material is available free of charge via the Internet at http://pubs.acs.org.

References and Notes

(1) Westheimer, F. H. *Science* **1987**, *235*, 1173−1178.
(2) Cox, J. R.; Ramsay, O. B. *Chem. Rev.* **1964**, *64*, 317−351.
(3) Bunton, C. A. *Acc. Chem. Res.* **1970**, *3*, 257−265.
(4) Thatcher, G. R. J.; Kluger, R. *Adv. Phys. Org. Chem.* **1989**, *25*, 99−265.
(5) Hodges, R. V.; Sullivan, S. A.; Beauchamp, J. L. *J. Am. Chem. Soc.* **1980**, *102*, 935−938.

(6) Lum, R. C.; Grabowski, J. J. *J. Am. Chem. Soc.* **1992**, *114*, 8619−8627.
(7) Asubiojo, O. I.; Brauman, J. I.; Levin, R. H. *J. Am. Chem. Soc.* **1977**, *99*, 7707−7708.
(8) Florián, J.; Warshel, A. *J. Phys. Chem. B* **1998**, *102*, 719−734.
(9) Dejaegere, A.; Liang, X.; Karplus, M. *J. Chem. Soc., Faraday Trans.* **1994**, *90*, 1763−1770.
(10) Chang, N.; Lim, C. *J. Phys. Chem. A* **1997**, *101*, 8706−8713.
(11) Hu, C.; Brinck, T. *J. Phys. Chem. A* **1999**, *103*, 5379−5386.
(12) Bianciotto, M.; Barthelat, J.-C.; Vigroux, A. *J. Am. Chem. Soc.* **2002**, *124*, 7573−7587.
(13) Goldstein, B. J. *Tyrosine Phospoprotein Phosphatases*, 2nd ed.; Oxford University Press: Oxford, NY, 1998.
(14) Jackson, M. D.; Denu, J. M. *Chem. Rev.* **2001**, *101*, 2313−2340.
(15) McComb, R. B. *Alkaline Phosphatases*, 1st ed.; Plenum Press: New York, 1979.
(16) Coleman, J. E. *Annu. Rev. Biophys. Biomol. Struct.* **1992**, *21*, 441−483.
(17) Bunton, C. A.; Fendler, E. J.; Fendler, J. H. *J. Am. Chem. Soc.* **1967**, *89*, 1221−1230.
(18) Kirby, A.; Varvoglis, A. *J. Am. Chem. Soc.* **1968**, *89*, 415−423.
(19) Hoff, R. H.; Hengge, A. C. *J. Org. Chem.* **1998**, *63*, 6680−6688.
(20) Friedman, J.; Freeman, S.; Knowles, J. *J. Am. Chem. Soc.* **1988**, *110*, 1268−1275.
(21) Menegon, G.; Loos, M.; Chaimovich, H. *J. Phys. Chem. A* **2002**, *106*, 9078−9084.
(22) Ayala, P.; Schlegel, H. B. *J. Chem. Phys.* **1998**, *108*, 2314−2325.
(23) Florián, J.; Åqvist, J.; Warshel, A. *J. Am. Chem. Soc.* **1998**, *120*, 11524−11525.
(24) Boldyrev, A.; Gutowski, M.; Simons, J. *Acc. Chem. Res.* **1996**, *29*, 497−502.
(25) Taylor, P. R. Accurate calculations and calibration. In *Lectures Notes in Quantum Chemistry−European Summer School in Quantum Chemistry*; Roos, B. O., Ed.; Springer-Verlag: Berlin, 1992; Vol. 1.
(26) Mercero, J. M.; Barrett, P.; Lam, C. W.; Fowler, J. E.; Ugalde, J. M.; Pedersen, L. G. *J. Comput. Chem.* **2000**, *21*, 43−51.
(27) Miller, B. *J. Am. Chem. Soc.* **1962**, *84*, 403−409.
(28) Dantzman, C. L.; Kiessling, L. L. *J. Am. Chem. Soc.* **1996**, *118*, 11715−11719.
(29) Cleland, W. W.; Hengge, A. C. *FASEB J.* **1995**, *9*, 1585−1594.
(30) Barford, D.; Das, A. K.; Egloff, M. P. *Annu. Rev. Biophys. Biomol. Struct.* **1998**, *27*, 133−164.
(31) Ditchfield, R.; Hehre, W.; Pople, J. A. *J. Chem. Phys.* **1971**, *54*, 724−728.
(32) Møller, C.; Plesset, M. S. *Phys. Rev.* **1934**, *46*, 618.
(33) Helgaker, T.; Jørgensen, P.; Olsen, J. *Molecular Electronic-Structure Theory*, 1st ed.; Wiley: New York, 2000.
(34) Schlegel, H. B. *Adv. Chem. Phys.* **1987**, *67*, 249−286.
(35) Krishnan, R.; Binkley, J.; Seeger, R.; Pople, J. *J. Chem. Phys.* **1980**, *72*, 650−654.
(36) Guthrie., R. D.; Jencks, W. P. *Acc. Chem. Res.* **1989**, *22*, 343−349.
(37) Bright Wilson, Jr., E.; Decius, J. C.; Cross, P. C. *Molecular Vibrations. The Theory of Infrared and Raman Vibrational Spectra*, 1st ed.; Dover: Ney York, 1980.
(38) Ochterski, J. W. "White paper: Vibrational analysis in Gaussian", Guassian Inc., 1999 http://www.Gaussian.com.
(39) McQuarrie, D. A. *Statistical Mechanics*, 1st ed.; Harper and Row: New York, 1976.
(40) Hehre, W. J.; Radom, L.; Schleyer, P. R.; Pople, J. A. *Ab Initio Molecular Orbital Theory*, 1st ed.; Wiley: New York, 1986.
(41) Fukui, K. *Acc. Chem. Res.* **1981**, *14*, 363−368.
(42) Gonzalez, C.; Schlegel, H. B. *J. Phys. Chem.* **1990**, *94*, 5523−5527.
(43) Szabo, A.; Ostlund, N. *Modern Quantum Chemistry*; Dover: New York, 1st ed.; 1989.
(44) Frisch, M. J.; et al. *Gaussian 98*, revision A.9; Gaussian Inc.: Pittsburgh, PA, 1998.
(45) Schaefer, A.; Horn, H.; Ahlrichs, R. *J. Chem. Phys.* **1992**, *97*, 2571−2577.
(46) Dunning, T. *J. Chem. Phys.* **1989**, *90*, 1007−1023.
(47) Ahlrichs, R.; Ber, M.; Hser, M.; Horn, H.; Klmel, C. *Chem. Phys. Lett.* **1989**, 165−169.
(48) 2004, http://www.dinamicas.art.br/quim/fosf.html.
(49) Arantes, G. M. On the protein tyrosine phosphatases. Phosphate esters intrinsic reactivity and computer simulation of the mechanisms of enzymatic reaction. Thesis, Institute of Chemistry, University of São Paulo, 2004.
(50) Osborn, D.; Leahy, D.; Kim, E.; deBeer, E.; Neumark, D. *Chem. Phys. Lett.* **1998**, *292*, 651−655.
(51) Gunion, R.; Gilles, M.; Polak, M.; Lineberger, W. *Int. J. Mass Spectrom. Ion Processes* **1992**, *117*, 601−620.
(52) Schwartz, R.; Davico, G.; Lineberger, W. *J. Electron Spectrosc. Relat. Phenom.* **2000**, *108*, 163−168.
(53) Hirschfelder, J. O.; Meath, W. J. *Adv. Chem. Phys.* **1967**, *12*, 3−106.
(54) Curtiss, L. A.; Redfern, P. C.; Smith, B. J.; Radom, L. *J. Chem. Phys.* **1996**, *104*, 5148−5152.
(55) Pulay, P.; Hamilton, T. *J. Chem. Phys.* **1988**, *88*, 4926−4933.
(56) Van, Duijneveldt, F. B.; Van, de Rijdt, J. G. C. M.; Van, Lenthe, J. H. *Chem. Rev.* **1994**, *94*, 1873−1885.
(57) Lendvay, G.; Mayer, I. *Chem. Phys. Lett.* **1998**, *297*, 365−373.
(58) Gryzyska, P.; Czyryca, P.; Golithtly, J.; Small, K.; Larsen, P.; Hoff, R.; Hengge, A. *J. Org. Chem.* **2002**, *67*, 1214−1220.
(59) Dubourg, A.; Roques, R.; Germain, G.; Declercq, J.; Garrigues, B.; Boyer, D.; Munoz, A.; Klaebe, A.; Comtat, M. *J. Chem. Res. (S)* **1982**, *7*, 180−181.
(60) Westheimer, F. H. *Acc. Chem. Res.* **1968**, *1*, 70−78.
(61) Parr, R. G.; Yang, W. *Density-Functional Theory of Atoms and Molecules*, 1st ed.; Oxford University Press: Oxford, 1996.
(62) Chang, N. Y.; Lim, C. *J. Am. Chem. Soc.* **1998**, *120*, 2156−2167.
(63) Take the difference between the relative energies of the TS for alcoholysis on carbon in the CH_3O^- + TMP reaction and of the C:IMC1. In ref 10, C:TS1 is described as TS-6, with $\Delta E_T = \Delta E_{MP2} + \Delta ZPE = -12.7$ kcal/mol, but ΔE_T of the IMC is not reported.
(64) Khan, S.; Kirby, A. *J. Chem. Soc. B* **1970**, 1172−1182.
(65) The diffusional barrier can be estimated as 3.2 kcal/mol on the basis of the value of the difussion constant ($k_d = 10^{10}$ s^{-1}).
(66) Åqvist, J.; Kolmodin, K.; Florián, J.; Warshel, A. *Chem. Biol.* **1999**, *6*, R71−R80.
(67) Santoro, E. *Org. Mass Spectrom.* **1973**, *7*, 589−600.
(68) George, L.; Sankaran, K.; Viswanathan, K.; Mathews, C. *Appl. Spectrosc.* **1994**, *48*, 7−12.
(69) Vidya, V.; Sankaran, K.; Viswanathan, K. S. *Chem. Phys. Lett.* **1996**, *258*, 113−117.
(70) Ballard, R. E.; Jones, J.; Read, D.; Inchley, A.; Cranmer, M. *Chem. Phys. Lett.* **1987**, *137*, 125−129.
(71) Nelson, R.; Lide, D.; Maryott, A. *Natl. Stand. Ref. Data Ser.* **1967**, *10*, 1.
(72) Robin, M.; Kuebler, N. *J. Electron Spectrosc. Relat. Phenom.* **1972**, *1*, 13−28.
(73) Less, R.; Baker, J. *J. Chem. Phys.* **1968**, *48*, 5299−5318.
(74) Lias, S.; Bartmess, J.; Liebman, J.; Holmes, J.; Levins, R.; Mallard, W. *J. Phys. Chem. Ref. Data* **1988**, *17*, 1−816 (Suppl. 1).
(75) Harmony, M.; Laurie, V.; Kuczkowski, R.; Schwendeman, R.; Ramsay, D.; Lovas, F.; Lafferty, W.; Maki, A. *J. Phys. Chem. Ref. Data* **1979**, *8*, 619−722.